

Broad electrical tuning of plasmonic nanoantennas at visible frequencies

Thang B. Hoang^{1,2} and Maiken H. Mikkelsen^{1,2,3,a)}

¹Department of Physics, Duke University, Durham, North Carolina 27708, USA

²Center for Metamaterials and Integrated Plasmonics, Duke University, Durham, North Carolina 27708, USA

³Department of Electrical and Computer Engineering, Duke University, Durham, North Carolina 27708, USA

(Received 11 February 2016; accepted 22 April 2016; published online 6 May 2016)

We report an experimental demonstration of electrical tuning of plasmon resonances of optical nanopatch antennas over a wide wavelength range. The antennas consist of silver nanocubes separated from a gold film by a thin 8 nm polyelectrolyte spacer layer. By using ionic liquid and indium tin oxide coated glass as a top electrode, we demonstrate dynamic and reversible tuning of the plasmon resonance over 100 nm in the visible wavelength range using low applied voltages between -3.0 V and 2.8 V. The electrical potential is applied across the nanoscale gap causing changes in the gap thickness and dielectric environment which, in turn, modifies the plasmon resonance. The observed tuning range is greater than the full-width-at-half-maximum of the plasmon resonance, resulting in a tuning figure of merit of 1.05 and a tuning contrast greater than 50%. Our results provide an avenue to create active and reconfigurable integrated nanophotonic components for applications in optoelectronics and sensing. © 2016 Author(s). All article content, except where otherwise noted, is licensed under a Creative Commons Attribution (CC BY) license (<http://creativecommons.org/licenses/by/4.0/>). [<http://dx.doi.org/10.1063/1.4948588>]

Metallic nanoparticles smaller than the wavelength of light can support localized surface plasmons and confine light in a region beyond the diffraction limit with greatly increased local density of states enabling applications from superresolution imaging^{1,2} to biosensing^{3,4} and photodetectors.^{5–9} Additionally, embedding light emitting materials in such sculpted electromagnetic environments allows for tailored light–matter interactions, including lasing,^{10,11} ultrafast spontaneous emission,¹² Purcell factors greater than 1000 (Ref. 13), and 30 000-fold photoluminescence enhancements.¹⁴ However, typically in order to modify the plasmon resonance, and thus the operating wavelength, the physical dimensions of the nanostructures have to be changed. To enable real-time reconfigurable optoelectronic and sensing applications, there has been a long quest for dynamically tunable plasmonic structures, and a variety of approaches have been explored. For example, previous schemes have employed temperature induced phase changes in materials such as germanium antimony telluride ($\text{Ge}_2\text{Sb}_2\text{Te}_5$)^{15,16} and vanadium oxide (VO_2) to modify the plasmon resonances,¹⁷ or have utilized microfluidics devices that enable plasmonic structures to be surrounded by liquids with varying index of refraction.¹⁸ Plasmonic nanostructures have also been fabricated on stretchable elastomeric films in order to modify the physical structures under compression and tension.¹⁹ However, for on-chip integration and future practical applications, electrical tunability is highly desirable. While there have been several recent demonstrations of electrical tuning of plasmonic structures,^{20–27} they either show a very limited tuning range around 10 nm,^{21,22,25} are restricted to the infrared spectral region,^{20,23,24,27} or require the application of a large voltage ~ 100 V.²⁶

In this paper, we experimentally demonstrate electrical tuning of the plasmon resonance of an ensemble of

n nanopatch antennas from 613 nm to 713 nm by the application of a small external bias voltage of less than 3 V. The nanopatch antennas consist of colloiddally synthesized silver nanocubes with a side length of ~ 75 nm placed over a gold film with an 8 nm dielectric polymer spacer layer sandwiched in between. This structure supports a transmission line mode and highly enhanced electric fields in the gap region up to a 100-fold for the fundamental mode centered at 646 nm.^{14,28} Figure 1(a) shows the simulated near-field pattern for a 75 nm film-coupled nanocube revealing large field enhancements in the gap region. For these finite-element COMSOL simulations, an incident plane wave impinged at an angle of 67° (from normal axis) onto the nanocubes is used with an excitation wavelength of 535 nm. The fundamental mode has a dominant field in the direction perpendicular to the sample surface and a Fabry–Pérot resonance is induced by multiple reflections of a waveguide mode propagating parallel to the film resulting in maximum field enhancements along the edges and corners of the nanocubes. The resonance of these nanopatch antennas depends strongly on the size of the nanocubes and the thickness and properties of the dielectric spacer material.^{9,28} For example, a change in the gap thickness of only 4 nm, from 1 to 5 nm, results in a large shift of the plasmon resonance from 1007 nm to 720 nm.⁹ Here, for a fixed nanocube size, the resonance of the nanopatch antennas is actively tuned by the application of an external bias voltage. To apply an electrical potential across the nanoscale gap region an indium tin oxide (ITO) coated glass slide in combination with ionic liquid is used as the top electrode and the gold film is used as the bottom electrode. The experimentally observed dynamic tuning over a wide wavelength range is believed to be the result of swelling, de-swelling and other voltage-dependent modifications to the polymer layer in the gap region between the silver nanocube and the gold film.

^{a)} Author to whom correspondence should be addressed. Electronic mail: m.mikkelsen@duke.edu



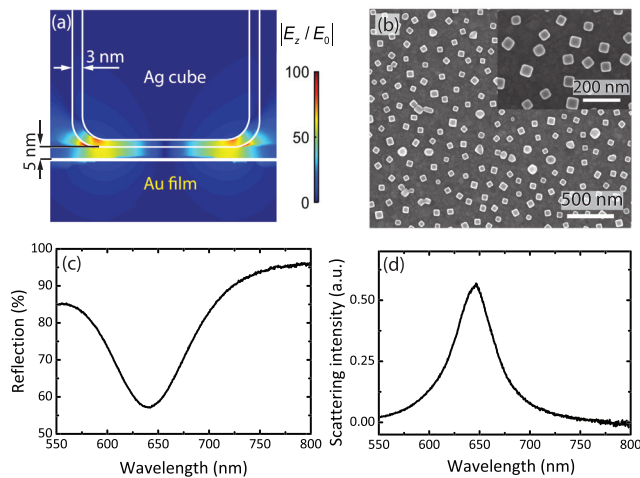


FIG. 1. Properties and characterization of nanopatch antennas. (a) Schematic of a nanopatch antenna consisting of a 50 nm gold (Au) film, a 5 nm polyelectrolyte spacer layer, and a ~ 75 nm silver nanocube with a 3 nm PVP polymer shell. The near field distribution of the transverse electric field of the fundamental plasmonic gap mode obtained from finite-element COMSOL simulations is also shown. Maximum field enhancements are observed near the corners of the nanocube. (b) SEM image of colloidal synthesized silver nanocubes with a typical side length of ~ 75 nm. The slightly rounded corners of the nanocubes are visible in the higher magnification SEM image shown in the inset. (c) Measured reflectivity spectrum from an ensemble of nanopatch antennas with a polymer gap size of 5 nm excluding the PVP shell around the nanocubes. (d) Representative dark-field scattering spectrum measured from an individual nanopatch antenna with a FWHM of 45 nm.

To fabricate the nanopatch antennas, 50 nm/5 nm Au/Cr films were evaporated onto commercially cleaned glass slides (Nexterion Glass B, SCHOTT North America, Inc.). A polymer spacer layer was formed by alternately submerging the gold coated glass slides in 3 mM poly(allylamine) hydrochloride (PAH) for 5 min and in 3 mM polystyrene sulfonate (PSS) for 5 min. The sample was rinsed with ultra-pure deionized water after each PAH or PSS layer and dried with clean nitrogen gas after the final polymer layer. The spacer layer both began and terminated with PAH to facilitate adhesion with the gold film and the silver nanocubes. The total thickness of the final 5 polyelectrolyte (PE) layers was measured by spectroscopic ellipsometer and determined to be 5.0 ± 0.1 nm in air. The silver nanocubes were chemically synthesized following previously published procedures.^{14,29,30} Scanning electron microscopy (SEM) was used to characterize the shape and size distribution of the nanocubes as seen in Fig. 1(b). From this, it was estimated that the synthesized nanocubes have a side length of 75 ± 10 nm and slightly rounded corners with a radius of curvature of ~ 10 nm, as seen in the inset in Fig. 1(b). As a result of the synthesis, the nanocubes are coated in a polyvinylpyrrolidone (PVP) layer with an estimated thickness of ~ 3 nm. For nanocube deposition, the samples were exposed to $50 \mu\text{l}$ of a concentrated nanocube solution (stock solution diluted 10 times) for 60 s. Silver nanocubes electrostatically adhered to the top PAH layer and resulted in a disperse nanocube surface coverage of $\sim 5\%$.

Optical characterization of the fabricated structures was performed by scattering and reflectivity measurements using optical dark-field microscopy. Reflectivity measurements from an ensemble of nanopatch antennas were performed

using a $5\times$, 0.15 NA objective, and scattering measurements of individual nanoantennas were performed using an extra-long working distance $50\times$, 0.55 NA objective. Figure 1(c) shows a typical reflectivity spectrum measured from an ensemble of nanopatch antennas displaying a plasmon resonance centered at 645 nm with a full-width at half maximum (FWHM) of 95 nm. The scattering spectra from individual nanopatch antennas are measured on samples with a lower density of nanocubes using the nanocube stock solution diluted 100 times for deposition. A representative scattering spectrum from an individual nanoantenna is shown in Fig. 1(d) with a FWHM of 45 nm. The width of the plasmon resonance is observed to be wider for ensembles of nanoantennas than for individual ones due to a small variation in the size of the silver nanocubes.

Next, in order to perform dynamic tuning of the plasmon resonance, we fabricate structures that enable an external voltage to be applied across the gap between the silver nanocubes and the underlying gold film shown schematically in Figs. 2(a) and 2(b). Spacer tape with a thickness of $\sim 100 \mu\text{m}$ and a $\sim 1 \text{ cm}^2$ round opening is placed on the nanopatch antenna sample described earlier. The volume created by the opening in the spacer tape is then filled with an electrically conductive ionic liquid (Sigma-Aldrich, 98.5% transmission, 500 ppm water impurity) and covered by an ITO coated glass slide (Delta Technologies Ltd.). This enables electrical contact to be made between the ITO and the nanocubes, serving as the top electrode, while the bottom gold film serves as the other electrode. A photograph of one of the fabricated sample structures is shown in Fig. 2(c). This sample consists of three structures: (i) two structures with integrated nanocubes as described earlier (seen as the two darker circular regions on the left in Fig. 2(c)), and (ii) a structure fabricated as described earlier but without any nanocubes used as a control sample and for normalization purposes (seen as the lighter circular region on the right in Fig. 2(c)). The electrical wires

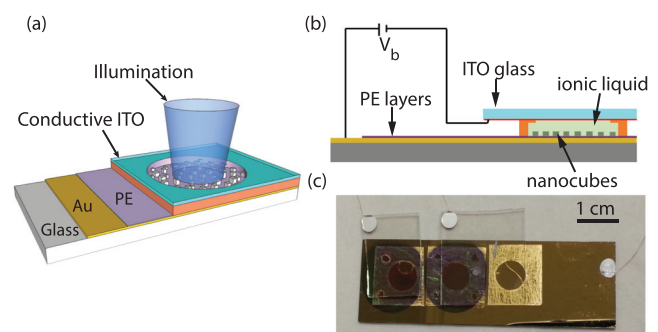


FIG. 2. Device structure for electrical tuning of plasmon resonances. (a) Schematic of the sample design consisting of silver nanocubes separated from a gold film by a thin polyelectrolyte (PE) spacer layer. An approximately 1 cm^2 area of the sample is isolated using spacer tape, creating a circular opening filled with an ionic liquid and subsequently covered by an ITO coated glass slide. Reflectivity spectra of the nanopatch antennas are measured from the top through the ITO coated glass slide. (b) Schematic cross-section of the sample structure is shown including electrical contacts. (c) Photograph of a fabricated structure with three devices. The spacer tape containing ionic liquid within the circular openings is seen along with the ITO coated slides used for electrical contacts. The two devices on the left consist of the structure as illustrated in (a) and (b), whereas the right device is the same structure but without any nanocubes and is used for normalization purposes.

are also seen which are attached with silver paint to the gold film and the underside of the glass slide which is coated by ITO.

To apply a DC voltage to the structure, a Yokogawa GS200 power supply is used and the current is monitored by a Keithley 6485 pico-ammeter. The structure acts as a capacitor and there is a small current due to charging and discharging. This small current also ensures a charge flow that maintains the gradient of the ion concentration in the liquid.^{31,32} Fig. 3(a) displays reflectivity spectra from an ensemble of nanopatch antennas taken at different applied voltages. The reflectivity spectrum was first measured at 0 V revealing a plasmon resonance at 630 nm. An external voltage of 2.8 V was then applied, and the reflectivity spectrum shows a resonance at 613 nm for this bias (top panel of Fig. 3(a)). Next, the external bias was removed and the device was set to short circuit in order to discharge the accumulated charges at the two electrodes. The reflectivity measurement at 0 V was then repeated and showed a resonance at 625 nm, essentially unchanged from the original resonance position considering the broad linewidth of the resonance. Subsequently, a reverse bias of -3.0 V was applied to the structure, and the reflectivity spectrum showed that the resonance was significantly red-shifted to 713 nm. Finally, once the external bias was removed again and the structure discharged, the measured reflectivity spectrum displayed a resonance at 620 nm, which is very close to the original resonance. This demonstrates that the tuning of the plasmon resonance is indeed reversible for the structure. The applied bias voltages were chosen such as to stay within the electrical window of the ionic liquid which is from -3.5 to 3.0 V. Even with this small range of applied bias, a large tuning range of 100 nm was achieved. The tuning of the plasmon resonance occurred on a relatively fast time scale of ~ 10 s. For the experiments described above, the measurement of each reflectivity spectrum was conducted with a 10-min waiting time after each voltage was turned on or off.

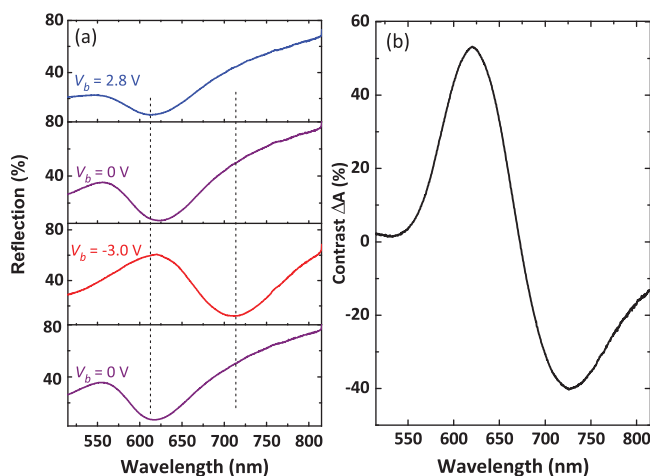


FIG. 3. Dynamic tuning of the plasmon resonance. (a) Reflectivity spectra of an ensemble of nanopatch antennas measured at different applied bias voltages, V_b , as indicated. The experimental sequence performed is shown from the top to the bottom panel. The dashed lines indicate the 100 nm tuning window of the plasmon resonance. The applied bias voltages are chosen such as to stay well within the electrical window of the ionic liquid from -3.5 to 3.0 V. (b) Extracted change in absorption at -3.0 V with respect to the absorption at 0 V.

In order to quantify the resonance switching of our plasmonic tuning device we estimated the tuning figure of merit which is defined as the ratio between the tuning range and the FWHM of the resonance.^{33,34} For the structure measured in Fig. 3(a), the tuning figure of merit is 1.05, which is the largest value reported for electrical tuning of plasmonic nanoantennas in the visible spectral region. Our observed value is comparable with the previously reported value of 1.03 for a mid-infrared antenna³⁴ and significantly larger than that for a tunable near-infrared metamaterial based on VO_2 phase transition, where a value of 0.14 was observed.³³ Additionally, we extracted the difference in the absorption,³⁵ or contrast, of the device under a bias voltage with respect to the absorption at zero voltage. As seen in Fig. 3(c), a contrast greater than 50% in the absorption is observed at a wavelength of ~ 620 nm.

To provide insight into the tuning mechanism, we consider possible modifications that may occur to the polyelectrolyte layers under an applied bias voltage. First, the combination of ionic liquid and polyelectrolyte layers may lead to swelling and de-swelling of the polyelectrolytes. Previously, it has been shown that depending on the concentration and stability of the ionic liquid, swelling of the polyelectrolyte layers can occur and may in some cases not be reversible.³⁶ Second, incorporation of ionic liquid with polyelectrolyte layers may not only change the thickness of the spacer layer but may also modify its effective dielectric constant.³⁶ Third, a potential-dependence of the ion density and structure of the ionic liquid near the metal electrodes may modify the resonance.^{36,37} Recently, a significant modification of the density and exchange of ions has been observed in an ionic liquid near a gold electrode during potential scans.³⁸ It is possible that this may affect the silver nanocubes in our experiments here, as the nanocubes are exposed to the ionic liquid and the potential is modulated by the bottom Au film electrode due to the applied bias voltage. Therefore, there is a possibility that the density and distribution of the ions near the surface of the nanocubes might be modulated, leading to changes in the dielectric environment around the nanocubes. However, this effect is expected to be diminished by the 3 nm PVP polymer layer surrounding the nanocubes. Fourth, the applied bias voltage may cause a charge accumulation layer at the surface of the top electrode due to injection of carriers into the ITO.²⁰ Finally, there is the possibility that oxidation of the nanocubes and the ITO layer from the top electrode could lead to modification of the plasmonic structure and environment.³⁹

To elucidate which of these possible mechanisms are dominating, we investigate whether the sample is modified by the exposure to the ionic liquid and the applied bias voltage. SEM images of the sample before and after the tuning experiment were performed are shown in Figs. 4(a) and 4(b), respectively. After the tuning experiment, the shape of the silver nanoparticles does not appear to have been modified; however, small features are observed to have emerged on the sample surface indicating that modifications have likely occurred to the polyelectrolyte layers. From analysis of many such SEM images, we find that the sizes of the cubes were 71 ± 8 nm before and 69 ± 7 nm after exposure to the ionic liquid confirming that no significant size change has

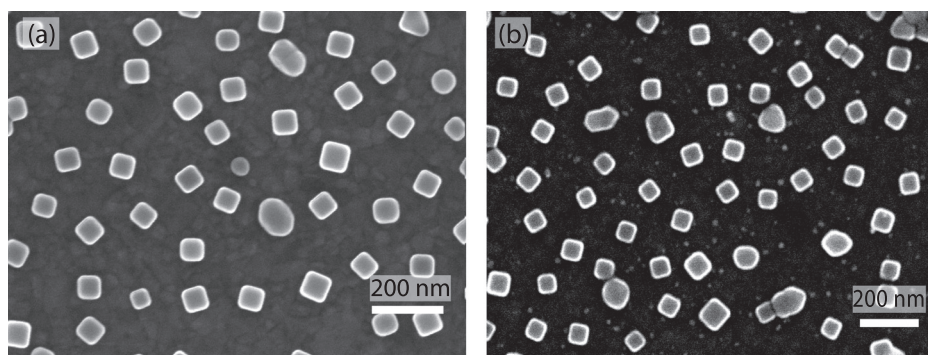


FIG. 4. Sample morphology before and after tuning. (a) SEM image of a sample with nanocube antennas before exposure to the ionic liquid and the applied bias voltage. (b) SEM image of the same sample after the tuning experiment was performed and the sample had been exposed to the ionic liquid and the applied bias voltage.

occurred. Additionally, recent experiments and simulations have shown that for a fixed gap size, a small 5 nm variation in the nanocube size only modifies the resonance wavelength by ~ 14 nm,²⁸ whereas a 2 nm change in the gap thickness has been shown to result in a resonance change of more than 100 nm.⁹ Furthermore, modifications to the index of refraction of the material in the gap region may also modify the plasmon resonance; however, recent studies have shown this effect to be much less significant than changes in the gap thickness.⁴⁰ Based on these observations, the tuning of the plasmon resonance observed in our experiment is most likely caused by the swelling and de-swelling of the polyelectrolyte layers depending on the polarity of the electric field and the highly concentrated ionic liquid in combination with a modified dielectric constant of the spacer layer. In turn, these modifications to the thickness and dielectric constant of the material in the gap between the metal film and the silver nanocubes lead to a modified plasmon resonance of the sample structure.^{21,40}

As seen from Fig. 3, a negative bias voltage is observed to induce a much larger shift in the plasmon resonance than a positive bias. This can be explained by a negative bias causing de-swelling of the polyelectrolyte layers, and thus a red shift of the resonance, whereas a positive bias causes swelling of the polyelectrolyte layers, and thus a blue shift of the resonance.^{28,40,41} As mentioned earlier, the relationship between the gap thickness and the plasmon resonance of the nanopatch antennas has previously been characterized and a non-linear dependence was observed.^{9,28,40} At small gap sizes of less than ~ 5 nm, the plasmon resonance has been observed to be extremely sensitive to changes in the gap size whereas at larger gaps, the plasmon resonance is much less sensitive. This is consistent with our observations here where de-swelling of the polyelectrolyte layers induces a larger shift in the plasmon resonance than swelling. The magnitude of the observed shift in the plasmon resonance of 100 nm is also consistent with these previous experiments where samples were fabricated with different gap thicknesses and a red shift of 104 nm was observed as the gap was changed from 5 nm to 3 nm (for 75 nm cubes).⁹

After the bias voltage is turned off, ideally the ionic liquid will become depolarized and any changes to the polyelectrolyte layers reversed. However, the charge regulation of the ionic liquid and the underlying polyelectrolyte layers may be slow and the induced modifications to the polyelectrolyte layers have been observed to not always be fully

reversible.^{36,37,42} This effect may explain the small variations in the plasmon resonance measured at a bias voltage of 0 V in between blue- and red-shifting the resonance, as well as causing some studied devices to not be fully reversible. As we have mentioned earlier, the tuning speed of the plasmon resonance in our device was ~ 10 s. This is due to the involvement of the ionic liquid and might not be ideal for applications that require a fast switching speed. In addition to this, the use of ionic liquid may also lead to a combination of complex interactions, such as chemical modifications to the polyelectrolyte layers, the top ITO electrode, or the nanocubes, which might be irreversible in some cases. While further work is required to explore such interactions in detail, the experiments presented here demonstrate the feasibility of dynamically tuning the plasmon resonance of nanopatch antennas over a wide wavelength range.

In summary, we demonstrated dynamic and reversible tuning of the plasmon resonance of nanopatch antennas over a 100-nm range in the visible spectrum. This was realized by applying a bias voltage across a polyelectrolyte spacer layer separating silver nanocubes from a gold ground plane, which in turn modifies the gap and thus the plasmon resonance of the structure. This dynamic tuning scheme could be integrated with, for example, semiconductor quantum dots,¹² two dimensional materials,⁴³ or even single emitters⁴⁴ for real-time control of absorption and spontaneous emission.

This work was supported by the Air Force Office of Scientific Research Young Investigator Research Program (AFOSR, Grant No. FA9550-15-1-0301). The authors thank Britt Lassiter and Gleb Akselrod for fruitful discussions.

¹M. Rycenga, X. Xia, C. H. Moran, F. Zhou, D. Qin, Z.-Y. Li, and Y. Xia, *Angew. Chem., Int. Ed.* **50**, 5473 (2011).

²S. M. Stranahan and K. A. Willets, *Nano Lett.* **10**, 3777 (2010).

³J. N. Anker, W. P. Hall, O. Lyandres, N. C. Shah, J. Zhao, and R. P. Van Duyne, *Nat. Mater.* **7**, 442 (2008).

⁴D. Rodrigo, O. Limaj, D. Janner, D. Etezadi, F. J. García de Abajo, V. Pruneri, and H. Altug, *Science* **349**, 165 (2015).

⁵S. Linic, P. Christopher, and D. B. Ingram, *Nat. Mater.* **10**, 911 (2011).

⁶J. A. Fan, C. Wu, K. Bao, J. Bao, R. Bardhan, N. J. Halas, V. N. Manoharan, P. Nordlander, G. Shvets, and F. Capasso, *Science* **328**, 1135 (2010).

⁷G. Konstantatos and E. H. Sargent, *Nat. Nanotechnol.* **5**, 391 (2010).

⁸Y. Liu, R. Cheng, L. Liao, H. Zhou, J. Bai, G. Liu, L. Liu, Y. Huang, and X. Duan, *Nat. Commun.* **2**, 579 (2011).

⁹G. M. Akselrod, J. Huang, T. B. Hoang, P. T. Bowen, L. Su, D. R. Smith, and M. H. Mikkelsen, *Adv. Mater.* **27**, 8028 (2015).

- ¹⁰Y.-J. Lu, J. Kim, H.-Y. Chen, C. Wu, N. Dabidian, C. E. Sanders, C.-Y. Wang, M.-Y. Lu, B.-H. Li, X. Qiu, W.-H. Chang, L.-J. Chen, G. Shvets, C.-K. Shih, and S. Gwo, *Science* **337**, 450 (2012).
- ¹¹M. T. Hill, Y.-S. Oei, B. Smalbrugge, Y. Zhu, T. de Vries, P. J. van Veldhoven, F. W. M. van Otten, T. J. Eijkemans, J. P. Turkiewicz, H. de Waardt, E. J. Geluk, S.-H. Kwon, Y.-H. Lee, R. Notzel, and M. K. Smit, *Nat. Photonics* **1**, 589 (2007).
- ¹²T. B. Hoang, G. M. Akselrod, C. Argyropoulos, J. Huang, D. R. Smith, and M. H. Mikkelsen, *Nat. Commun.* **6**, 7788 (2015).
- ¹³G. M. Akselrod, C. Argyropoulos, T. B. Hoang, C. Ciraci, C. Fang, J. Huang, D. R. Smith, and M. H. Mikkelsen, *Nat. Photonics* **8**, 835 (2014).
- ¹⁴A. Rose, T. B. Hoang, F. McGuire, J. J. Mock, C. Ciraci, D. R. Smith, and M. H. Mikkelsen, *Nano Lett.* **14**, 4797 (2014).
- ¹⁵X. Yin, M. Schäferling, A.-K. U. Michel, A. Tittl, M. Wuttig, T. Taubner, and H. Giessen, *Nano Lett.* **15**, 4255 (2015).
- ¹⁶A.-K. U. Michel, P. Zalden, D. N. Chigrin, M. Wuttig, A. M. Lindenberg, and T. Taubner, *ACS Photonics* **1**, 833 (2014).
- ¹⁷Y. Abate, R. E. Marvel, J. I. Ziegler, S. Gamage, M. H. Javani, M. I. Stockman, and R. F. Haglund, *Sci. Rep.* **5**, 13997 (2015).
- ¹⁸A. Yang, T. B. Hoang, M. Dridi, C. Deeb, M. H. Mikkelsen, G. C. Schatz, and T. W. Odom, *Nat. Commun.* **6**, 6939 (2015).
- ¹⁹F. Huang and J. J. Baumberg, *Nano Lett.* **10**, 1787 (2010).
- ²⁰F. Yi, E. Shim, A. Y. Zhu, H. Zhu, J. C. Reed, and E. Cubukcu, *Appl. Phys. Lett.* **102**, 221102 (2013).
- ²¹J. J. Mock, R. T. Hill, Y.-J. Tsai, A. Chilkoti, and D. R. Smith, *Nano Lett.* **12**, 1757 (2012).
- ²²C. Novo, A. M. Funston, A. K. Gooding, and P. Mulvaney, *J. Am. Chem. Soc.* **131**, 14664 (2009).
- ²³J. Kim, H. Son, D. J. Cho, B. Geng, W. Regan, S. Shi, K. Kim, A. Zettl, Y.-R. Shen, and F. Wang, *Nano Lett.* **12**, 5598 (2012).
- ²⁴Y. Yao, M. A. Kats, R. Shankar, Y. Song, J. Kong, M. Loncar, and F. Capasso, *Nano Lett.* **14**, 214 (2014).
- ²⁵K. C. Chu, C. Y. Chao, Y. F. Chen, Y. C. Wu, and C. C. Chen, *Appl. Phys. Lett.* **89**, 103107 (2006).
- ²⁶J. Müller, C. Sönnichsen, H. von Poschinger, G. von Plessen, T. A. Klar, and J. Feldmann, *Appl. Phys. Lett.* **81**, 171 (2002).
- ²⁷Y. Yao, M. A. Kats, P. Genevet, N. Yu, Y. Song, J. Kong, and F. Capasso, *Nano Lett.* **13**, 1257 (2013).
- ²⁸J. B. Lassiter, F. McGuire, J. J. Mock, C. Ciraci, R. T. Hill, B. J. Wiley, A. Chilkoti, and D. R. Smith, *Nano Lett.* **13**, 5866 (2013).
- ²⁹Q. Zhang, W. Li, L.-P. Wen, J. Chen, and Y. Xia, *Chem. A Eur. J.* **16**, 10234 (2010).
- ³⁰T. B. Hoang, J. Huang, and M. H. Mikkelsen, "Colloidal synthesis of nanopatch antennas for applications in plasmonics and nanophotonics," *J. Visualized Exp.* (to be published, 2016).
- ³¹D. Daghero, F. Paolucci, A. Sola, M. Tortello, G. A. Ummaino, M. Agosto, R. S. Gonnelli, J. R. Nair, and C. Gerbaldi, *Phys. Rev. Lett.* **108**, 066807 (2012).
- ³²H. Yuan, H. Shimotani, J. Ye, S. Yoon, H. Aliah, A. Tsukazaki, M. Kawasaki, and Y. Iwasa, *J. Am. Chem. Soc.* **132**, 18402 (2010).
- ³³M. J. Dicken, K. Aydin, I. M. Pryce, L. A. Sweatlock, E. M. Boyd, S. Walavalkar, J. Ma, and H. A. Atwater, *Opt. Express* **17**, 18330 (2009).
- ³⁴A.-K. U. Michel, D. N. Chigrin, T. W. W. Maß, K. Schönauer, M. Salinga, M. Wuttig, and T. Taubner, *Nano Lett.* **13**, 3470 (2013).
- ³⁵M. S. Jang, V. W. Brar, M. C. Sherrott, J. J. Lopez, L. Kim, S. Kim, M. Choi, and H. A. Atwater, *Phys. Rev. B* **90**, 165409 (2014).
- ³⁶N. Parveen and M. Schönhoff, *Macromolecules* **46**, 7880 (2013).
- ³⁷A. G. Cherstvy, *J. Phys. Chem. B* **118**, 4552 (2014).
- ³⁸K. Motobayashi, K. Minami, N. Nishi, T. Sakka, and M. Osawa, *J. Phys. Chem. Lett.* **4**, 3110 (2013).
- ³⁹X. Zhang, E. M. Hicks, J. Zhao, G. C. Schatz, and R. P. Van Duyne, *Nano Lett.* **5**, 1503 (2005).
- ⁴⁰A. W. Powell, D. M. Coles, R. A. Taylor, A. A. R. Watt, H. E. Assender, and J. M. Smith, *Adv. Opt. Mater.* **4**, 634 (2016).
- ⁴¹A. Moreau, C. Ciraci, J. J. Mock, R. T. Hill, Q. Wang, B. J. Wiley, A. Chilkoti, and D. R. Smith, *Nature* **492**, 86 (2012).
- ⁴²N. Nishi, Y. Hirano, T. Motokawa, and T. Kakiuchi, *Phys. Chem. Chem. Phys.* **15**, 11615 (2013).
- ⁴³G. M. Akselrod, T. Ming, C. Argyropoulos, T. B. Hoang, Y. Lin, X. Ling, D. R. Smith, J. Kong, and M. H. Mikkelsen, *Nano Lett.* **15**, 3578 (2015).
- ⁴⁴T. B. Hoang, G. M. Akselrod, and M. H. Mikkelsen, *Nano Lett.* **16**, 270 (2016).